sustainability

MDPI

Article

Heat and Moisture Relevant In Situ Measurements in a Railway Passenger Vehicle Driving through the Swiss Alpine Region

Wolfgang Raedle, K. Ghazi Wakili *, Christoph Geyer, Roman Hausammann and Urs Uehlinger

Institute for Timber Construction, Structures and Architecture, Bern University of Applied Sciences (BFH), Solothurnstrasse 102, 6, CH-2500 Biel, Switzerland; wolfgang.raedle@bfh.ch (W.R.); christoph.geyer@bfh.ch (C.G.); roman.hausammann@bfh.ch (R.H.); urs.uehlinger@bfh.ch (U.U.)
* Correspondence: karim.ghaziwakili@bfh.ch; Tel.: +41-32-344-03-75

Abstract: Transportation is a major sector of energy consumption in most, if not in all, European countries. Besides the energy used for traction, energy is also consumed for ventilation, heating, and cooling inside the vehicles to assure traveler comfort. This issue gains increasing importance as the demand for public transport increases in the future. There is a need for retrofit to improve the thermal resistance of the envelope of existing vehicles to reduce the heat loss to the environment during the cold period of the year, especially in the Alpine region. A major concern in adding insulation material to the envelope is the possibility of convective moisture transfer due to air circulation in the vehicle, which would cause condensation accumulation on the cold surfaces. The present investigation addresses this topic by measuring surface and air temperature, air moisture, air flow, and heat flow at several critical locations of a vehicle during its travel in the Swiss Alpine region over several months during the cold period of the year. Temperature measurements showed the potential of reducing the heat losses in some parts of the vehicle. The level and duration of the moisture exposure did not suggest a relevant formation of condensation in the cross-section of the vehicle wall. The observed increase in relative humidity when driving through tunnels is too short to cause relevant condensation in the vehicle shell. The measured low air flow justifies the assumption that no forced convection occurs in the envelope cavities.

Keywords: railway vehicle; in situ measurement; vehicle envelope; moisture transfer; retrofit; heat loss

Citation: Raedle, W.; Wakili, K.G.; Geyer, C.; Hausammann, R.; Uehlinger, U. Heat and Moisture Relevant In Situ Measurements in a Railway Passenger Vehicle Driving through the Swiss Alpine Region. *Sustainability* **2022**, *14*, 7462. https://doi.org/10.3390/su14127462

Academic Editors: Pietro Evangelista, Mladen Jardas, Predrag Brlek, David Brčić, Zlatko Sovreski and Ljudevit Krpan

Received: 25 April 2022
Accepted: 16 June 2022
Published: 18 June 2022

1. Introduction

In Switzerland, the primary sector in terms of energy consumption is transportation. It accounted for more than one third, or 37.7%, of energy consumption for 2020, with an increasing trend, according to the Swiss Federal Statistical Office [1]. Increasing population and encouragement of the government to use public transport will increase the demand in the future. Besides the energy used for traction, the main energy is consumed by ventilation, heating, and cooling required to provide a comfortable environment for travelers. It is straightforward that the envelope and the windows of the passenger vehicles have a decisive influence in this respect, as they are the barrier between the interior and exterior climates. Secondary factors are the cooling, heating, and ventilation aggregates responsible for keeping the interior climatic conditions in compliance with comfort requirements during the summer and the winter period.

The thermal transmittance of a vehicle envelope can be determined for steady state conditions, but in real use, it is dependent on many parameters, and it varies with them as they change over time. Air circulation within the envelope structure and moisture uptake of the insulation material, resulting in convective heat and mass transfer, are the most influential of these parameters. In mountainous regions, it is during the heating period (fall and winter) that the influence of these parameters becomes perceptible. Convective moisture transfer into the porous insulation material can cause condensation and at low

temperatures, even enable the formation of ice, which reduces the insulating property. Different insulation materials have different moisture uptake behaviors, which means that the knowledge of the hygrothermal conditions in the envelope is vital in the selection of the most appropriate insulation material for the vehicle envelope.

One of the earliest articles providing an overview of the current requirements for air conditioning systems in rail vehicles was by Haller [2]. In a detailed analysis of the comfort parameters based on the requirements of the respective standard EN 13129 [3], it presented all the possible ways of improving thermal comfort. It was designed as a guideline for railway operators, rail vehicle manufacturers, and manufacturers of air-conditioning systems.

Following the above standard [3], the climatological operating conditions for summer and winter are divided into three climatic zones, namely Southern Europe, Central Europe, and Northern Europe, shown in Table 1. The corresponding maximum air speed in the interior is also stated in the standard, depending on the local interior air temperature (Table 2).

Table 1. Design conditions for maximum mean interior temperature/relative humidity for main line rolling stock according to EN 13129-1 [3].

Climatic Zones			**T_{max}/rh $_{max}$**
Summer All seats occupied	I	+40 °C/40% rh; 800 W/m^2	+27 °C/51.6% rh
	II	+35 °C/50% rh; 700 W/m^2	+27 °C/51.6% rh
	III	+28 °C/45 % rh; 600 W/m^2	25.3 °C/57.5% rh
Winter With wind but without solar load	I	−10 °C	+22 °C
	II	−20 °C	+22 °C
	III	−40 °C	+22 °C

Table 2. Maximum air speed for main line rolling stock according to EN 13129-1 [3].

Local Interior Air Temperature T_i	**Max. Air Speed in the Interior**
+22 °C	0.25 m/s
+27 °C	0.60 m/s

A mathematic model to simulate the dynamic cooling load of an air-conditioned train compartment was proposed by Liu et al. [4], showing that calculating the dynamic cooling load can provide an adequate basis to determine the cooling load for trains traveling in different regions and seasons. Barone et al. [5] also proposed a dynamic simulation approach for energy, economic, and environmental impact, along with thermal comfort analyses.

A study focused on the transparent portion of the envelope has been reported by Bouvard et al. [6], where the impact of the solar gains on the HVAC energy consumption of a panoramic train (large windows) has been investigated. They showed that the incoming energy due to the solar gains is in the same order of magnitude as required for the heating or cooling systems, and that an appropriate choice of the glazing can lead to energy savings of 7 to 13%, depending on the climate.

Regarding heating and cooling in light rail vehicles, Beusen et al. [7] reported on a detailed monitoring campaign resulting in an optimized strategy, reducing the respective energy consumption under the climatic conditions of Flanders, Belgium. Chang et al. [8] have analyzed the energy use and environmental emissions of high-speed rail transportation in China, without elaborating on the envelope materials and their thermal properties. A study presented by Chow [9] dealing with the ventilation requirements in the train compartments of railway lines in Hong Kong found that to keep the carbon-dioxide level in the train compartment low, a high ventilation rate must be provided. Gonzalez-Gil et al. [10] reported that, without going more into detail, auxiliaries' energy consumption of a single

vehicle per passenger-km for a predefined duty cycle is one of 12 key performance indicators. A more elaborate investigation regarding the optimal control of thermal comfort in trams has been performed by Hofstädter et al. [11]. Here too, simple assumptions were made regarding the heat transfer through the envelope, without referring to effectively measured data. Lin et al. analyzed the thermal comfort of passengers in short- and long-haul vehicles by involving simultaneous physical measurements and a questionnaire survey, collecting data from 2129 respondents. They reported a neutral temperature of 27 °C and a corresponding comfort zone for both types of vehicles between 22 °C and 29 °C [12]. A model to simulate the dynamic evolution of the temperature inside an air-conditioned high-speed train compartment has been presented and investigated by Mastrullo et al., focusing mainly on refrigerant alternatives, but without any in situ measured data [13]. There are further surveys carried out regarding thermal comfort in rail cars [14], but without any measurements of temperature or relative humidity in different parts of the envelope to point out possible risks of condensation.

Powell et al. have shown in their comprehensive investigation that the energy consumed by stabled vehicles is not negligible compared to the energy consumption of vehicles in service, and found that about 11% of the yearly energy consumption is accounted for by on-board auxiliary systems while the vehicle is stabled. Heating has been shown to be responsible for about 45% of this consumption [15]. Finally, Wernery et al. evaluated the use of superinsulation materials in trains to reduce heating/cooling demand [16]. They screened and benchmarked selected commercially available superinsulation materials in terms of thermal conductivity, fire safety, behavior under vibration and preferred use position within the train envelope. A previous study [17] on modeling the energy balance of a Swiss railway wagon showed that 55% of the heat losses are experienced through the envelope of the wagon (transmission losses) and 37% through the exhaust air of the ventilation system. There was another study [18] which included the monitoring of six vehicles of four different railway companies during several years, in which the climatic processes in the cross-section of the vehicle envelope were also discussed, without investigating them in detail. The assumption in the mentioned study [18] was that the following relevant factors occur in the cross-section of the vehicle wall:

- Formation of condensation between the outer shell and the thermal insulation of rail vehicles;
- Ice formation between the outer shell and the thermal insulation of rail vehicles;
- Strong air currents between the inner lining and the thermal insulation due to pressure differences (between the passenger compartment and the outside climate) caused by the ventilation system of the rail vehicles.

It was not examined or proven whether these factors actually occur in the cross-section of a vehicle wall or not.

For answering these questions, the present study was based on heat and moisture relevant in situ measurements in a railway passenger vehicle for a period of 7 months during the cold season in the Swiss Alpine region. The measured data incorporated temperature, relative humidity, heat flow, and air flow at different critical parts of the vehicle and was recorded during the normal schedule of the train in this period of the year. This included stops, ingress and egress of passengers, and passages through tunnels on the way back and forth between the start and final stations. Based on the analysis of the measurements performed under real conditions, recommendations regarding the choice of insulating material and their positioning in the vehicle envelope have been formulated to reduce heat loss as a retrofit measure.

2. Measuring Equipment

Based on experience acquired during former research projects [17,18] dealing with energy efficient HVAC of railways passenger vehicles, a number of different sensor types were chosen for the present investigations to measure the following physical quantities:

- The temperature of the outside air;

- The relative humidity of the outside air;
- The temperature of the air in the passenger compartment;
- The relative humidity of the air in the passenger compartment;
- The surface temperature of the outer shell and the interior cladding;
- The air temperature between the outer shell and the thermal insulation and between the thermal insulation and the interior cladding;
- The relative humidity between the outer shell and the thermal insulation and between the thermal insulation and the interior cladding;
- The air speed between the interior cladding and the thermal insulation;
- The heat flux density through the vehicle wall;
- The pressure difference between the passenger compartment and the outside climate;
- The global radiation;
- The energy meter, heating output, convective heating, and the passenger compartment.

2.1. Selection of Sensor Types

The selected sensors used for the present investigation are summarized in Table 3.

Table 3. Summary of the characteristics of the sensors/equipment used in this investigation. The sensors belonging to the University of Basel, who kindly shared the measured data, are shown in gray.

Sensor/Equipment	Application Range	Accuracy	Supplier
Logger ALMEMO 5690-1		0.02%	Ahlborn
Modem ZA 1 709 GPRS			Ahlborn
Antenna GPS/GSM/UMTS/WLAN			Ahlborn
Temp/RH sensor FHAD46C0L05	−40 °C to 85 °C 5 to 98% rh	±0.4 K ±4%	Ahlborn
Thermocouple Type T	−200 °C to 400 °C		Ahlborn
Heat flow sensor FQAD18T	0–26/0–260 mV	± 5 %	Ahlborn
Thermal anemometer FVAD35TH5K1	0.2 to 20 m/s	+2%	Ahlborn
Temp/RH sensor CMa20 indoor	−20 °C to +55 °C 10% to 90% RH	±0.2°K ±2% RH	Elvaco
Temp/RH sensor CMa11 outdoor	−40 °C to +55 °C 0 to 100% R	±0.5°K ±2% RH	Elvaco
Pressure difference			
Solar Irradiation SP Lite 2	400 to 1100 nm	60 to 100 µV/W/m^2	Kipp & Zonen
GPS receiver EVK-6H			u-blox
Energy meter DIZ-D651	3 × 230/400 VAC	+15%, −20%	ELKO

2.2. Positioning and Installation of Sensors

Several group of sensors have been built into the envelope at 3 different positions, S1, S2, and S3 (Figure 1), and at 8 different sites of the vehicle (Figure 2). As the incoming fresh air enters the vehicle after passing over a heating register and the exhaust air leaves through the outer edges of the ceiling, there is no need to put sensors nearby those air circulations. Further, the floor area was not accessible. Stadler Rail (the constructor of the vehicle) has confirmed that this can only be opened with great effort. In addition, the radiators were located on the entire side of the car. For these reasons it was not necessary to install sensors in this area.

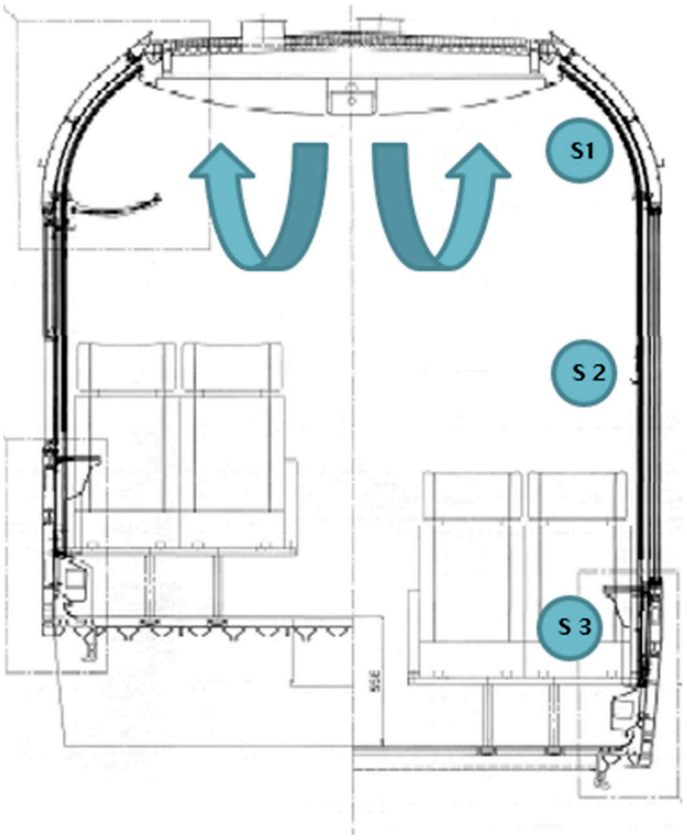

Figure 1. RhB BDT 1751-58 vehicle. Vertical positions S1, S2, and S3 of sensor groups in the vehicle envelope.

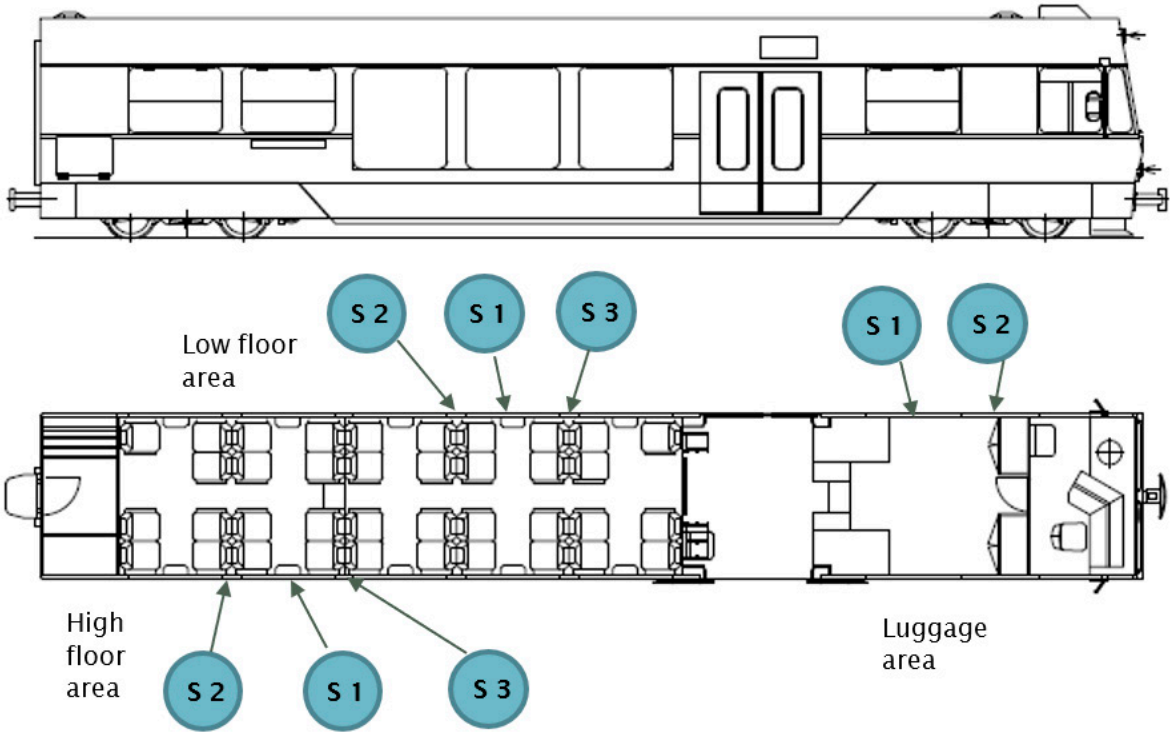

Figure 2. RhB BDT 1751-58 vehicle. Horizontal positions S1, S2, and S3 of the sensor groups in the vehicle envelope. These correspond to the positions in Figure 1.

With the introduction of the NEVA Retica timetable concept in November 1999, the Rhaetian Railway (RhB) put the BDt 1751-58 vehicle, built by Stadler Rail, into service. Various locomotives can be remotely controlled with these universal control cars. The vehicles approved for 100 km/h have a low-floor area between the bogies and a driver's brake valve to control the vacuum train brake; the cars themselves are braked by compressed air via a proportional valve. Since December 2004, three BDt vehicles have been running between Landquart and Davos, and another three between Pontresina and Scuol-Tarasp.

2.3. Sensor Group S1

The structure of this area consists of the external cladding made of extruded aluminum profiles, 40 mm thermal insulation, and an air cavity of 16 mm between the thermal insulation and the interior cladding made of glass reinforced plastic (GRP). The sensors of this group are shown in Figure 3.

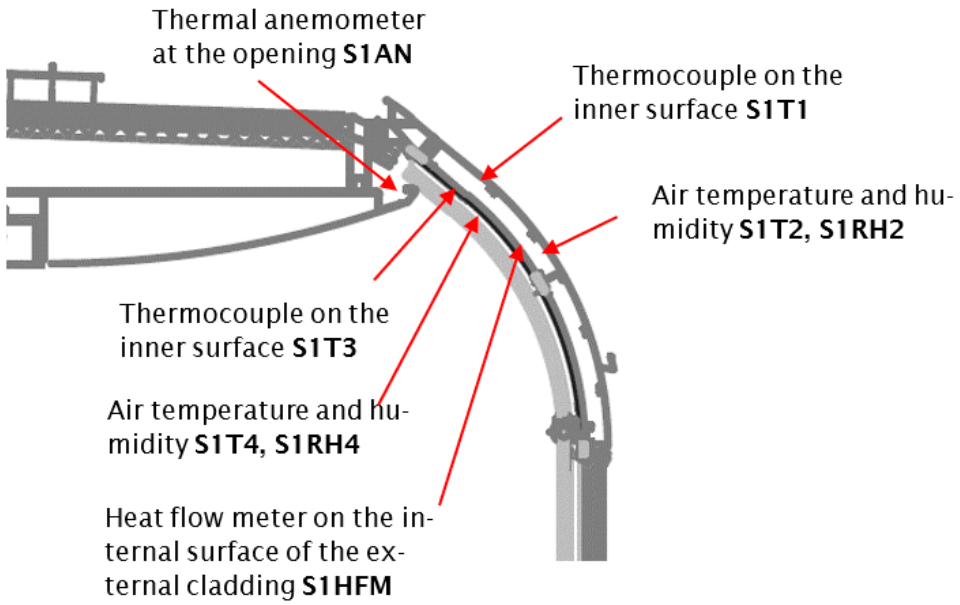

Figure 3. Type of sensors of Group S1 and their position in the vehicle.

2.4. Sensor Group S2

The structure of this area consists of the outer cladding made of extruded aluminum with hollow chamber profiles, 20 mm thermal insulation, and an air cavity of 16 mm between the thermal insulation and the interior cladding made of glass reinforced plastic (GRP). The insulation foam is compressible and can be slightly pressed by installing a heat flow plate for good contact. The sensors of this group are shown in Figure 4.

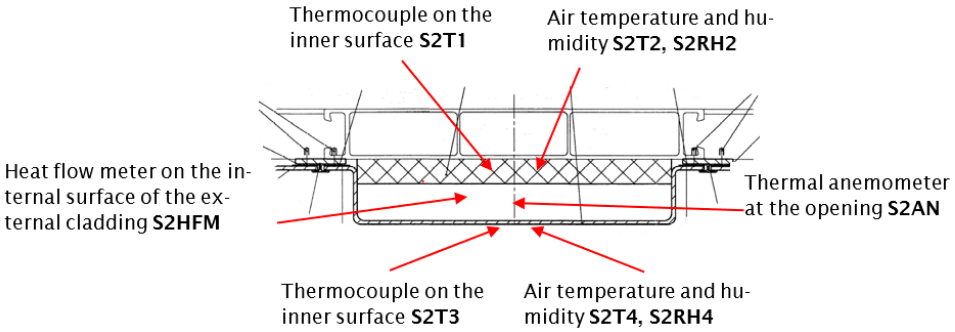

Figure 4. Type of sensors of Group S2 and their position in the vehicle.

2.5. Sensor Group S3

The structure of this area also consists of an aluminum exterior cladding (40 mm of thermal insulation with a vapor barrier and an air cavity of 16–19 mm) between the thermal insulation and the interior cladding. The insulation is compressible and can be pressed by installing a heat flow plate for good contact. The sensors of this group are shown in Figure 5.

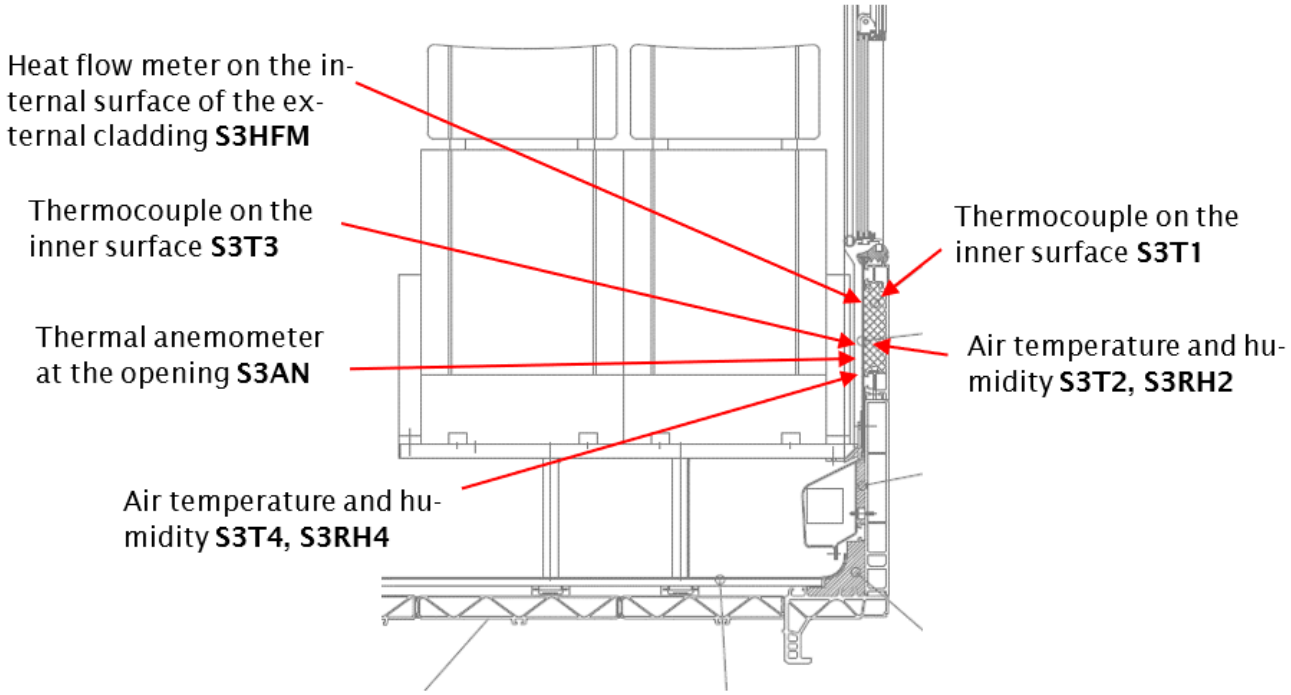

Figure 5. Type of sensors of Group S3 and their position in the vehicle.

2.6. Sensors for the Internal Air

There were four additional combined temperature and relative humidity sensors installed to measure the internal air in the compartments (**IT1, IRH1/IT2, IRH2/IT3, IRH3/IT4, IRH4**). They were positioned so that the measured values represent an average room climate during the monitoring period.

2.7. Sensor Installation

The thermocouples were fixed directly onto the outer shell with an aluminum adhesive tape towards the inner room. A combined temperature and moisture sensor was glued between the outer shell and the thermal insulation. It is important that the insulation is cut cleanly and fixed again after gluing the sensors, without any gaps or overlaps.

All other sensors were mounted using a frame with a bar (Figure 6). The whole unit was screwed or glued to the interior cladding. The bars in the frame are dimensioned in such a way that the heat flow plate is pressed lightly against the thermal insulation. This ensures a correct measurement of the heat flow without additional air gaps falsifying the results. The exact distance was determined by measuring the free space after the interior cladding had been dismantled.

Figure 6. Auxiliary construction for fastening the thermal anemometer (shiny metallic probe at the bottom), the heat flow plate (gray square), and the combined air temperature and relative humidity sensors (black) into their relative positions indicated in the previous figures.

This auxiliary construction has the following advantages:

The frame material is made of pine/epoxy resin (for better strength);
Recesses on the epoxy resin profile reduce the contact between the frame and the heat flow meter plate (Figure 6);
The measurement is not influenced by highly thermally conductive materials;
The heat flow through the aluminum cladding of the thermal insulation is reduced by the frame zone;
The complete unit can be attached or glued to the interior cladding with two screws;
The heat flow meter plate is pressed against the thermal insulation without gluing. The exact distance was adjusted to the specific proportions/dimensions by adjusting the bars before assembly;
Rounded frame edges reduce damage to the thermal insulation and the aluminum cladding.

2.8. Data Acquisition

The acquisition rate of the system is 0.1 s, so it needs less than 5 s for reading 48 sensors. The measured values are saved once per minute. The memory is deleted after successful data transfer.

2.9. GPRS Antenna, Pyranometer, and Sensors for External Air

With the exception of the GPRS Antenna, all other sensors belong to the University of Basel, who kindly shared the measured data for the evaluations in this investigation.

The mentioned sensors position on the outer back-face of the vehicle is shown in Figure 7.

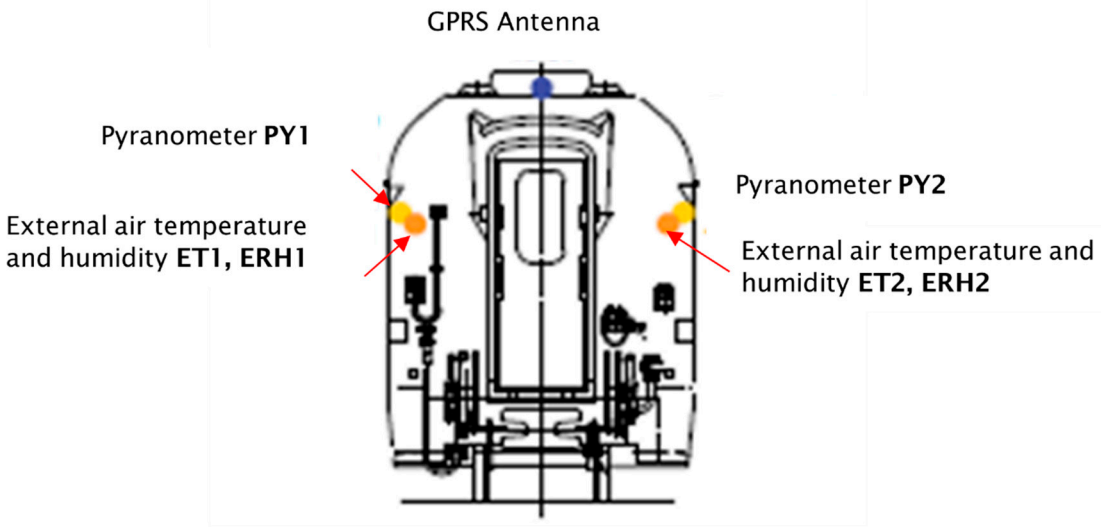

Figure 7. Position of sensors for temperature and relative humidity of the external air, the GPRS antenna and the two pyranometers on the outer back-face of the vehicle.

2.10. Power Supply

The power supply for the measuring equipment is ensured by the battery of the vehicle. The measuring system restarts automatically after a power failure. The system is therefore ready for operation again as soon as the vehicle is back in use.

2.11. The Path of the Vehicle

The route network of the Rhaetian Railway (the largest Alpine railway in Switzerland) is shown below in Figure 8. The route taken by the vehicle used for the present investigation is shown in red color. The route contains a long passage through the Vereina Tunnel, which shows an important impact on the measured data, as will be discussed later.

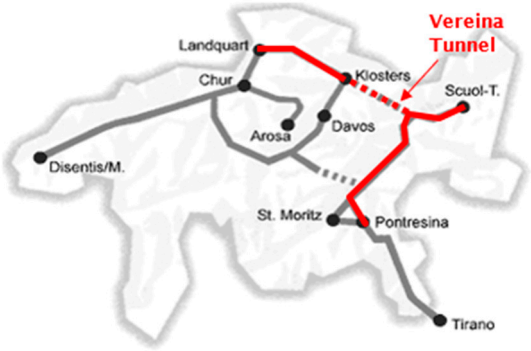

Figure 8. The path of the vehicle during the in situ measurements (in red).

3. Results and Discussion

In the following sections, a representative part of all data measured in the period beginning on 30 September 2017 and ending on 30 April 2018 (with a short gap of 20 days) are presented and analyzed. This time interval represents a typical winter period in the Swiss Alpine region. It is only during this period that climate-dependent and energy-relevant measurements can be collected, as the indoor and outdoor temperatures differ the most.

3.1. Temperature Measurements

A gap in the measured values was detected for the period from 18 December 2017 to 8 January 2018. Measured values were recorded during this time, but the transmission of the

data from the vehicle to our data server failed during this period, and the corresponding data was lost. Since we still have enough meaningful data for the evaluation period (October 2017 up to and including April 2018), the loss of data in the mentioned period does not pose a problem.

Figure 9 shows the measured external air temperature **ET1** for the period between 24 September 2017, and 6 May 2018, which represents the cold period of the year in the Swiss Alpine region.

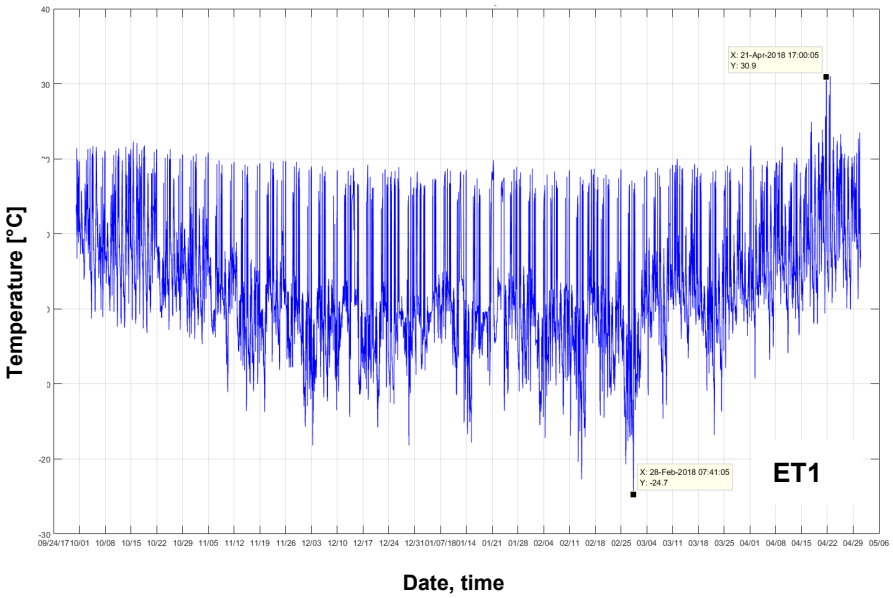

Figure 9. Measured external air temperature ET1 from 24 September 2017 to 6 May 2018.

In periods of generally low outside temperatures, we repeatedly measure short periods of outside temperatures above 10 °C. Figure 10 shows this effect as an example for 28 February 2018. A spot check showed that this effect can be assigned to the tunnel passages through the Vereina Tunnel and the Albula Tunnel.

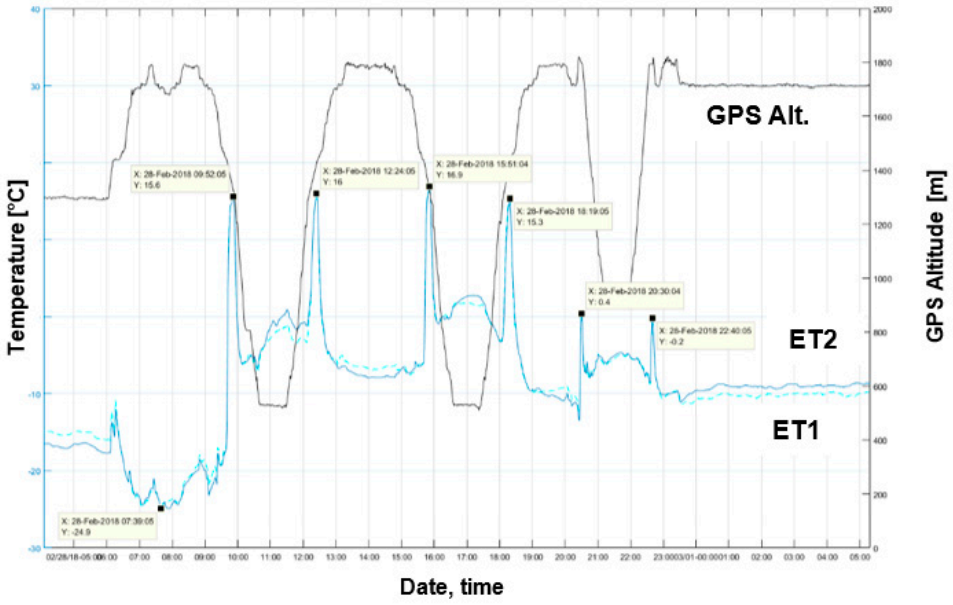

Figure 10. Measured external air temperature (**ET1 and ET2**, left *y*-axis) and GPS altitude (black, right *y*-axis) for the whole day of 28 February 2018.

09:52 a.m.: passage through the Vereina Tunnel in the direction of the Rhine Valley
12:25 p.m.: passage through the Vereina Tunnel in the direction of the Engadin
03:52 p.m.: passage through the Vereina Tunnel in the direction of the Rhine Valley
06:18 p.m.: passage through the Vereina Tunnel in the direction of the Engadin
08:30 p.m.: passage through the Vereina Tunnel in the direction of Tiefencastel
10:40 p.m.: passage through the Vereina Tunnel in the direction of the Engadin

There is a slight difference between the two sensors **ET1** and **ET2** (dotted and full blue lines in Figure 10). This might be due to several factors, such as different local exposure to wind flow, solar irradiation, ice formation, or sensor accuracy. As they are considered as negligible, their discrepancy will not be followed further.

Figure 11 shows that during the evaluation period, the air temperature **IT4** in the passenger compartment is slightly higher than the air temperature in the luggage compartment **IT2,** and fluctuates less. This can be explained by the fact that the luggage compartment has no partition to the vehicle door; thus, the outside air can flow unhindered into the luggage compartment when the door is opened. Further, Figure 11 shows the nighttime reduction in heating in both the passenger compartment and the luggage compartment. One can also see that the night reduction does not occur every night. This is due to shortcomings of the installation of relatively old control technology.

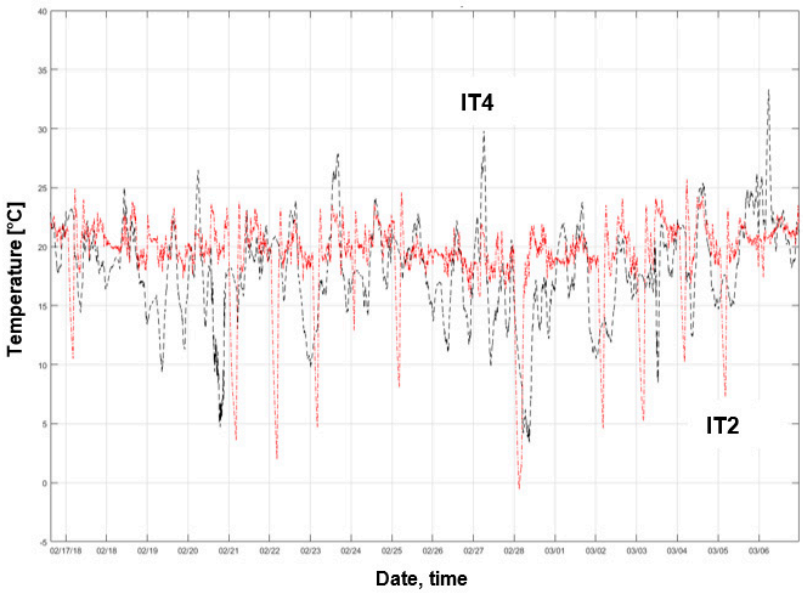

Figure 11. Measured air temperatures in the passenger room (IT4) and the luggage compartment (IT2) from 17 February to 6 March 2018.

The surface temperatures of the interior paneling beneath the window (see Figure 5) are very noticeable, both in the high-floor area and in the low-floor area. At room air temperatures in the range of 20 °C to 25 °C, we measure temperatures of up to 64.3 °C at these measuring points, whereas the temperatures in the low-floor area are somewhat higher than the temperatures in the high-floor area (Figure 12). These high surface temperatures are clearly related to the heat output of the convection heater (**HP** in Figure 12) in the passenger compartment.

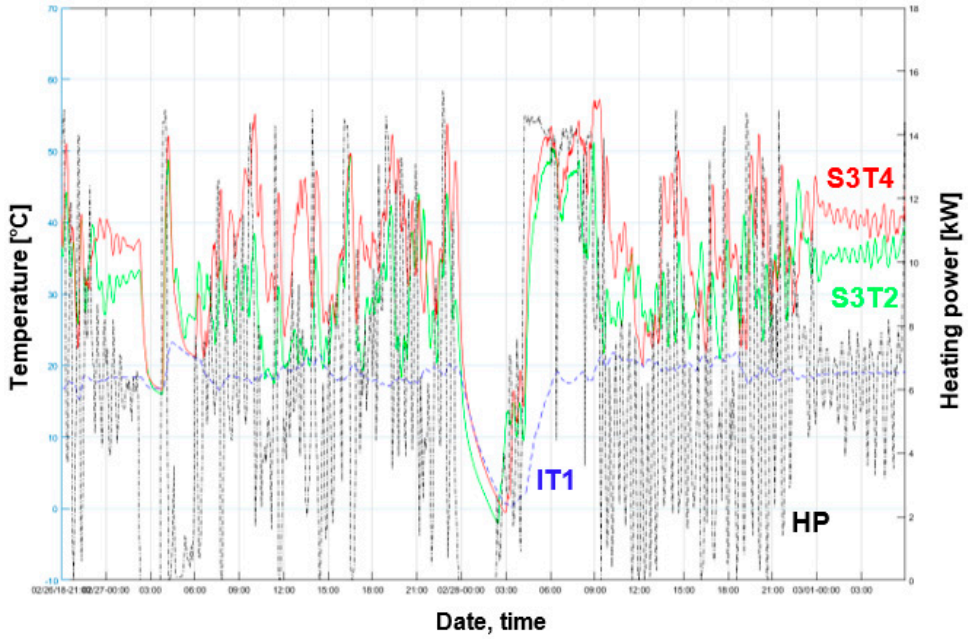

Figure 12. Measured air temperature in the passenger compartment **IT1** and beneath the window **S3T2** and **S3T4** (see Figure 5), as well as the heating power **HP**.

3.2. Humidity Measurements

Similar to the external air temperature sensors, the corresponding humidity sensors (ERH1, ERH2 in Figure 13) show slightly different values, which can be neglected in the further discussion of the results.

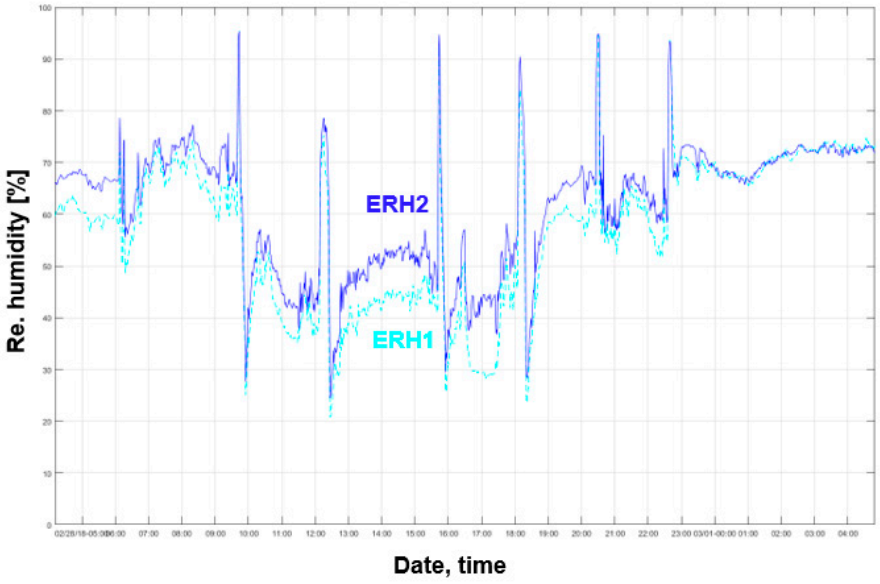

Figure 13. Measured relative humidity of the external air ERH1 and ERH2 (see Figure 7).

During the evaluation period, the relative humidity of the room air is generally low. Relative humidity greater than 50% in the room can only occur for a very short time; an accumulation of the relative humidity in the vehicle cannot be seen from the available measured data. Critical values for relative humidity are not reached in the evaluation period. The monthly mean values of air relative humidity shown in Table 4 illustrate the situation.

Table 4. Measured relative humidity of the internal air during the measuring period (MM—monthly mean value).

Month	IRH1			IRH2			IRH3			IRH4		
	Min.	Max.	MM	Min.	Max.	MM	Min.	Max.	MM	Min.	Max.	MM
October 2017	8.9%	74.3%	31.5%	10%	62.6%	30.9%	8.5%	68.7%	30.3%	0.1%	77.2%	29.3%
November 2017	10.9%	56.7%	25.4%	9.0%	50.3%	24.7%	8.0%	55.9%	24.1%	6.1%	62.6%	22.4%
December 2017	8.1%	72.1%	25.3%	8.3%	66.1%	23.6%	7.3%	71.9%	23.3%	4.4%	84.9%	20.9%
January 2018	10.3%	76.3%	29.2%	8.7%	68.9%	26.3%	8.0%	82.0%	25.6%	0.4%	73.5%	23.3%
Feberary 2018	7.4%	75.1%	23.3%	6.5%	60.0%	21.3%	5.2%	65.5%	20.2%	1.7%	68.3%	16.8%
March 2018	8.3%	67.8%	25.9%	8.1%	58.3%	23.9%	6.2%	68.8%	22.6%	1.1%	80.9%	20.4%
April 2018	9.5%	69.8%	30.0%	9.2%	61.7%	28.4%	8.1%	66.9%	27.6%	0.2%	74.6%	27.2%

The relative humidity at the measuring points in the passenger compartment (sensor humidity **IRH2** and sensor humidity **IRH3**) differs only slightly (Figure 14). The evolution of the two values also has similar characteristics. Slight deviations are to be expected due to air currents in the compartment, temperature stratification of the air horizontally and vertically, and different distances between the sensors, the compartment door, and the passengers.

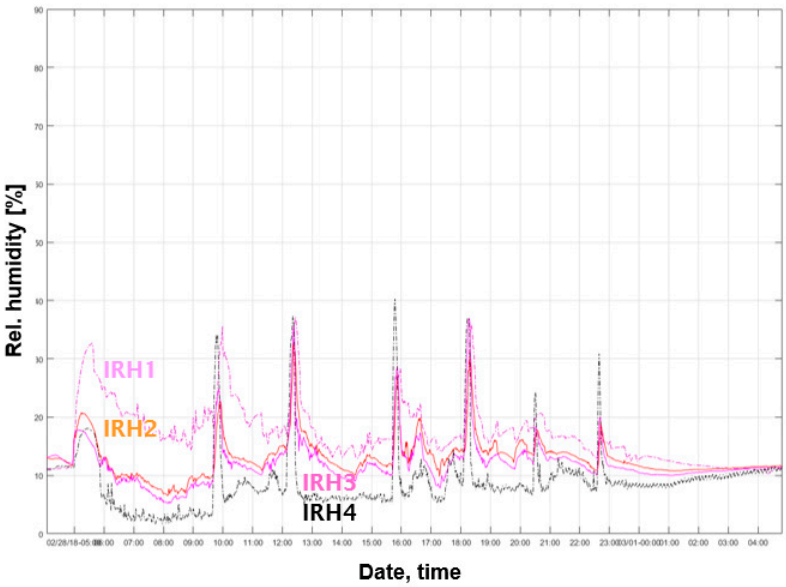

Figure 14. Measured relative humidity of the internal air IRH1, IRH2, IRH3, and IRH4.

The relative humidity in the luggage compartment (humidity sensor **IRH1**) differs significantly from the relative humidity in the passenger compartment (Figure 14). This can be explained due to the fact that the luggage compartment is directly exposed to the opening and closing of the outer door. The evolution of the relative humidity in the luggage compartment and in the passenger compartment differs in detail, but not fundamentally. This indicates that the relative humidity in the vehicle is massively influenced by the humidity of the outside air.

The relative humidity measured in the air duct (humidity sensor IRH4) also differs significantly from the relative humidity in the passenger compartment and in the luggage compartment (Figure 14). This can be explained by the fact that the air in the supply air duct comes directly from outside and has not yet been exposed to any influences in the passenger compartment. In the case of significant changes in humidity, however, the course of the measured values over time is very similar at all 4 measuring points. This indicates that the relative humidity in the vehicle is massively influenced by the humidity of the

outside air. It must be considered that different air temperatures with the same absolute humidity content of the air lead to different relative humidity values.

For the investigated period, we can assume that there was no relevant formation of condensation in the vehicle shell.

In the passenger compartment (high-floor area and low-floor area, see Figure 2), critical relative humidity (above 90%) is only reached at a few points for a short period of time, as can be seen in Figures 15 and 16. The roof area of the luggage compartment has the greatest potential for condensation to form. Here, the number and periods of conditions critical for condensation formation are more frequent and longer than in the passenger compartment (Figure 16). However, the number and duration of periods with critical conditions for condensate formation are also extremely low at this position.

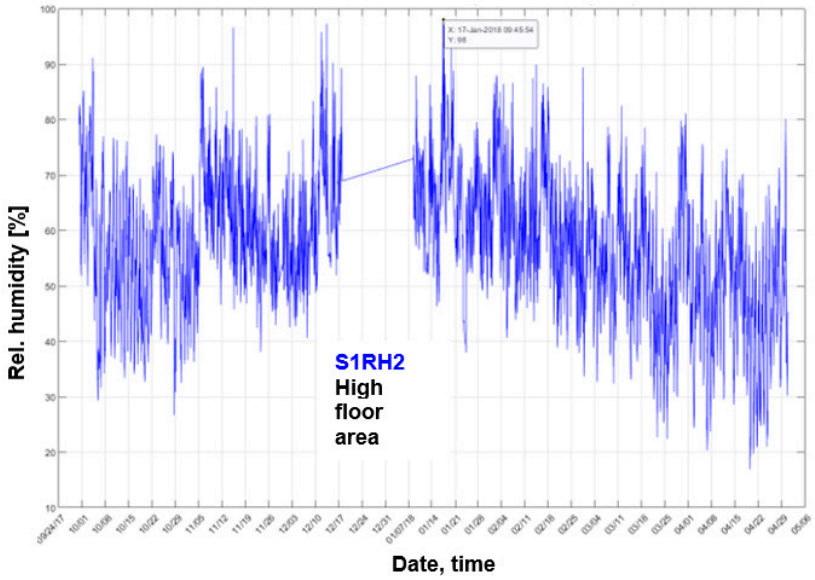

Figure 15. Measured relative humidity S1RH2 (see Figure 3) on the roof of the high floor area (see Figure 2) during the monitoring period, including the measurement gap mentioned previously (3.1).

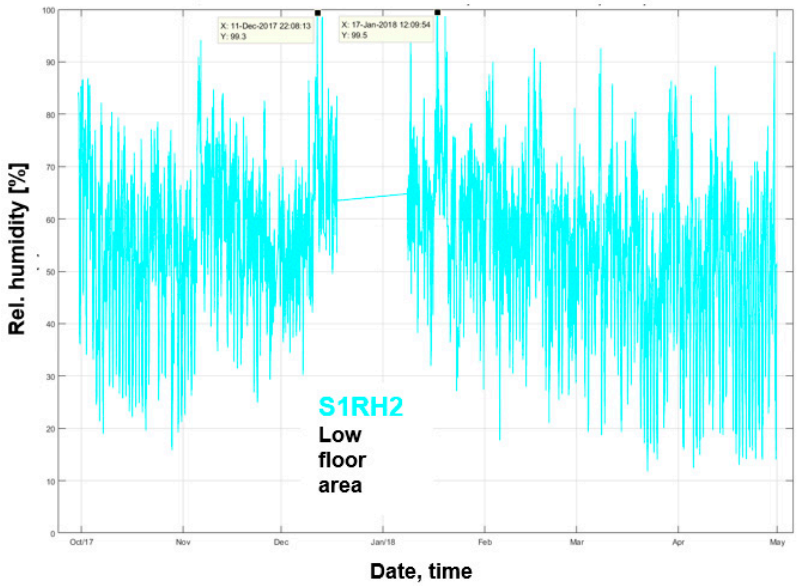

Figure 16. Measured relative humidity S1RH2 (see Figure 3) on the roof of the low floor area (see Figure 2) during the monitoring period, including the measurement gap mentioned previously (3.1).

Figure 17 shows that periods of critical moisture conditions are always followed by periods of significant drying. If condensation occurs at all at this measuring position, this is only short-term and does not lead to permanent moisture build-up at this position.

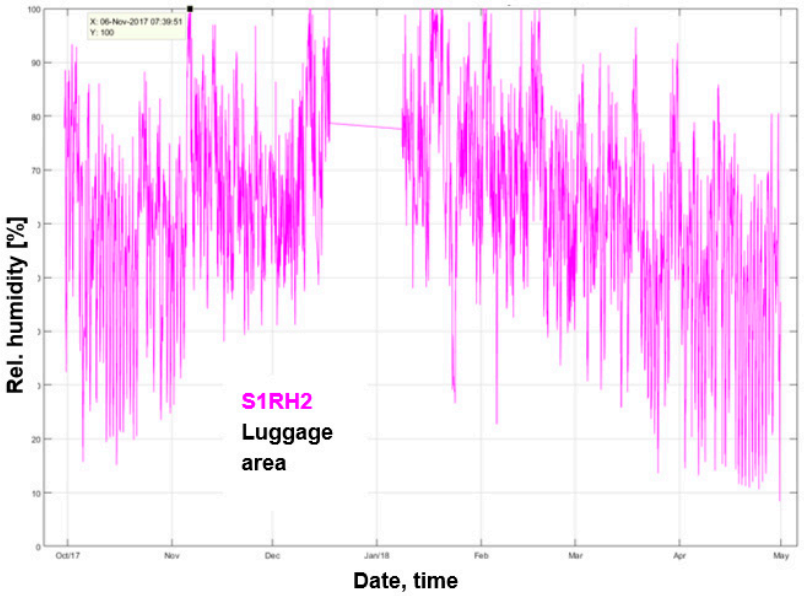

Figure 17. Measured relative humidity S1RH2 (see Figure 3) on the roof of the luggage area (see Figure 2) during the monitoring period, including the measurement gap mentioned previously (3.1).

At the measuring points where the relative humidity of the air layers close to the surface of the interior lining is measured **S1RH4**, **S2RH4,** and **S3RH4** (in Figures 3–5, respectively) we did not measure any values during the evaluation period that would indicate the formation of condensation on the interior lining (Figure 18). Here too, we measured values for relative humidity in the wall area above the windows, the luggage compartment, the low-floor area, and the high-floor area, in diminishing order.

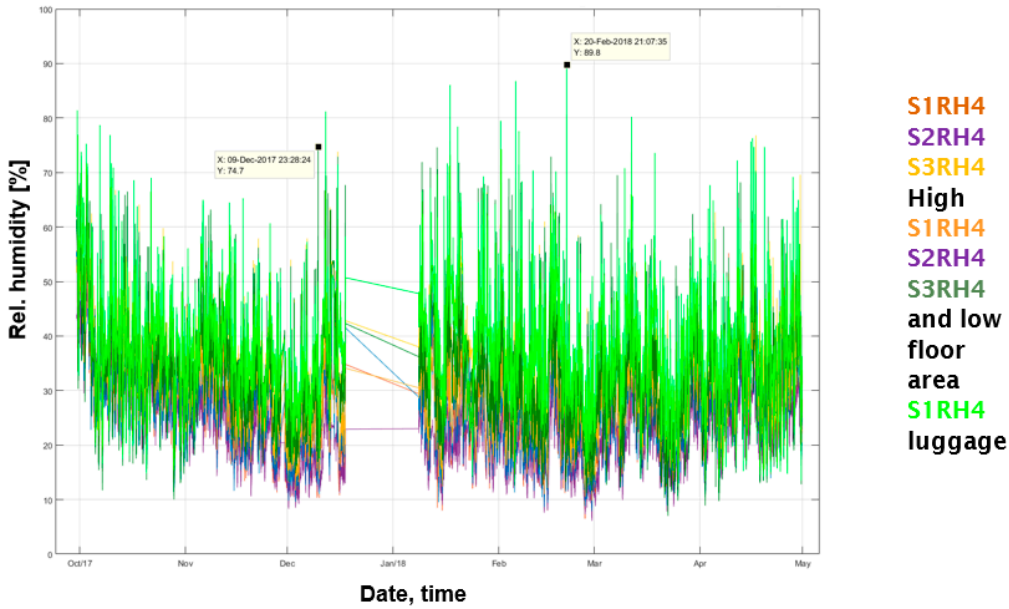

Figure 18. Measured relative humidity S1RH4 (Figure 3), S2RH4 (Figure 4), and S3RH4 (Figure 5) of the high and low floor areas (Figure 2) and in the luggage compartment during the monitoring period, including the measurement gap mentioned previously (3.1).

The attempt to find a correlation between the relative humidity in the passenger compartment and the occupancy, determined by measuring CO_2 concentration of the air in the passenger compartment, had a negative result. The relative humidity inside correlates with the relative humidity outside.

The passage through the tunnels (Vereina Tunnel and Albula Tunnel) led to an increase in the relative humidity in the vehicle wall, which varied in intensity at the different measuring points. The increase in relative humidity remained in a non-critical range (Figure 19).

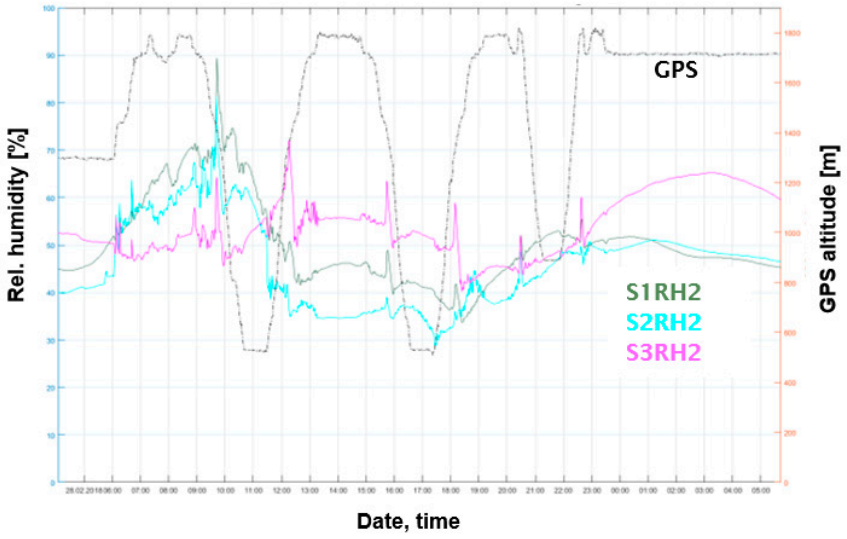

Figure 19. Measured relative humidity S1RH2 (Figure 3), S2RH2 (Figure 4), and S3RH2 (Figure 5) for 28 February 2018.

When driving through the Vereina Tunnel, peak relative humidity values of 100% occur in a few cases at the measuring points (Figure 20). These peak values occur only briefly (<0.5 h) and are always accompanied by a subsequent significant drop in relative humidity. A long-lasting moistening or an accumulation of moisture is not recognizable.

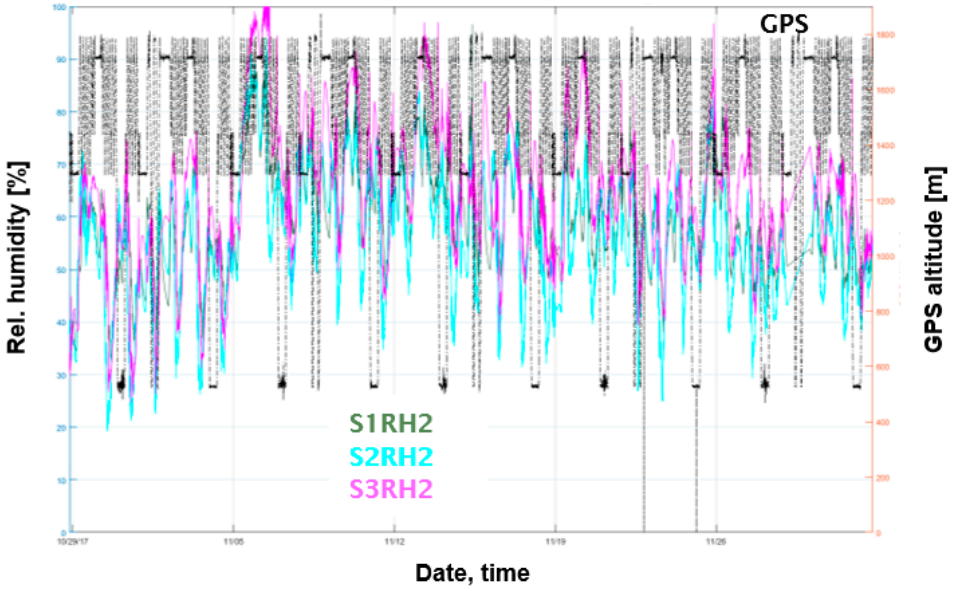

Figure 20. Measured relative humidity S1RH2 (Figure 3), S2RH2 (Figure 4), and S3RH2 (Figure 5) for November 2017.

In addition, the risk of condensation forming on the vehicle wall was checked by calculating the dew point temperature of the near-surface air layers for the individual measuring points. The surface temperature of the associated measuring point was then subtracted from the calculated dew point temperature. As long as the result is negative (surface temperature higher than the dew point temperature of the associated air layer), condensation can be ruled out. The evaluation of the dew point temperature leads to the same conclusions as the evaluation of the relative humidity reported above.

For the observation period, we can assume that there was no relevant formation of condensation in the vehicle shell.

3.3. Air Flow in the Vehicle

As Figure 21 shows, out of seven anemometers measuring air movements, only two showed some relevant values, and these lasted for only short periods of time between 4 and 10 min. This is a clear indication that no convection effects occur in the air cavities of the vehicle envelope; hence, no moisture transport is foreseeable from the warm interior to the cold surfaces.

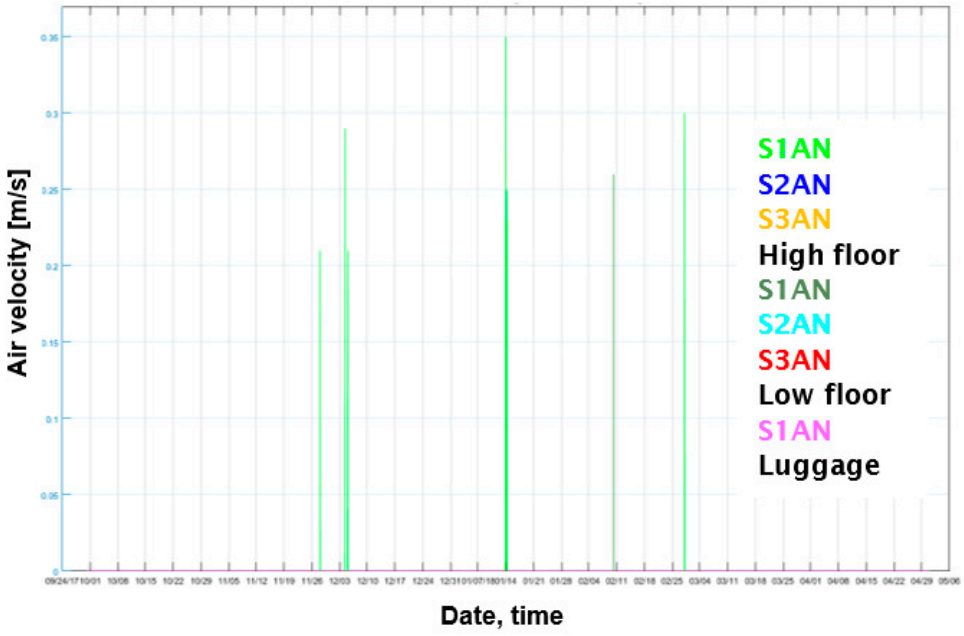

Figure 21. Measured air velocity by anemometers S1AN (Figure 3), S2AN (Figure 4), and S3AN (Figure 5) in the three areas: high floor, low floor, and luggage compartment (Figure 2).

3.4. Heat Flow through the Vehicle

A total of 8 heat flow plates, as shown in Figures 2–5, were attached to measure the heat flow densities in the high floor, low floor, and luggage compartments. Positive values for the heat flow density indicate heat gains via the vehicle wall at the measuring points for the heat flow density, and negative values for heat loss, correspondingly. Heat gains or heat losses through the vehicle shell are primarily caused by the temperature of the outside air.

The heat flux densities are close to each other in 5 of the 8 heat flow plates. We measure significantly increased heat flow densities with 3 heat flow plates (Figure 22).

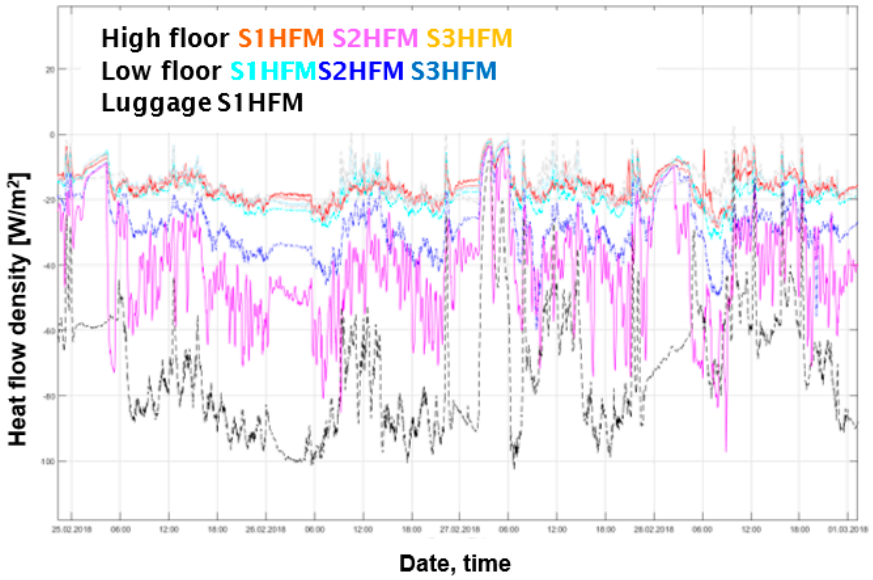

Figure 22. Measured heat flow densities S1HFM, S2HFM, and S3HFM through the vehicle walls (high floor, low floor, luggage compartment) for the period between 25 February 2018 and 1 March 2018.

Two heat flow plates with increased heat flow densities are located in the parapet area of the low-floor and high-floor areas (Figure 22). This corresponds to the temperatures measured in the high floor area (Figure 12) and our statement regarding increased heat losses at these points. A heat flux plate with a greatly increased heat flux density is located in the area next to the luggage compartment window (Figure 22). There was no immediate explanation for this high heat flow density from the measured temperatures. When installing the BFH measuring device, we found that the thermal insulation in this area was less thick than in the passenger compartment. This explains the deviating behavior with regard to the heat flow density at this measuring point.

4. Conclusions

4.1. Regarding Measured Temperatures

During the observation period, the measured outdoor temperatures were between +30.9 °C and −24.7 °C. Thus, a wide range of possible outdoor temperatures for the selected observation period has been covered by these measurements. These can be considered as representative for the winter and the transition period.

The short-term increase in outside temperature observed when driving through tunnels does not lead to any discernible problems with regard to the measured temperature inside the vehicle. However, the effects of the tunnel passages with regard to the air moisture in the vehicle and in the cross-section of the vehicle wall must be investigated.

The high temperatures on the interior cladding in the high floor area, in combination with the wall structure in this area, are a source of relevant heat losses. There is a potential of reducing the heat losses in this part of the vehicle

By using the night setback even more consistently, additional heating energy could be saved.

4.2. Regarding Measured Humidity

In the evaluation period from 29 September 2017 to 30 April 2018, we did not measure any values regarding the level and duration of the moisture exposure that would suggest a relevant formation of condensation in the cross-section of the vehicle wall. Moisture penetration into the thermal insulation can be excluded based on these measurements.

The absolute humidity at all measuring points, i.e., the outside air, the room air, and the air in the cross-section of the vehicle shell, is basically the same. In situations in where the values diverge, they converge again very quickly. Apparently, the humidity of the outside

air determines the humidity in the interior and in the cross-section of the vehicle shell. This indicates an intensive exchange of moisture (vapor pressure equalization) between the outside climate, the interior climate, and the cross-section of the vehicle wall. Possible causes for this are frequent door openings, a vehicle envelope that is leaky in terms of vapor pressure equalization, air exchange through the ventilation system (maximum approx. 950 m^3/h), or a combination of these factors.

The observed increase in relative humidity when driving through tunnels is too short to cause relevant condensation in the vehicle shell. In addition, the increase in humidity in the tunnels is accompanied by an increase in temperature. This also reduces the risk of condensation.

The vehicle is mainly on the road in the Engadine (a mountainous region in Southeast Switzerland). The climate in the Engadine tends to be cold, which also leads to low absolute humidity. A location with different climatic conditions may lead to different results with regard to condensation.

The observations made initially only apply to the type of vehicle under consideration. It is not clear to what extent these can be transferred to other types of vehicles with a more modern envelopes.

4.3. Regarding Measured Air Flow

The differential pressure does not lead to any forced convection in the cross-section of the vehicle envelope. This means that there is no need for solutions with convection barriers for selecting the prototype concepts for the retrofit of the envelope. The measured air velocities can be traced back to natural (not forced) convection. The fact that natural convection occurs in gas-filled cavities is not disputed and does not have to be investigated further. The low air flow justifies the assumption that we are dealing with unventilated cavities, in this case.

Based on this result, the use of IR reflective layers should be considered when selecting the prototype concepts and the planned laboratory tests. Some preliminary numerical simulations have been carried out showing that the U-value (thermal transmittance) of the wall cross-section without an IR reflective layer of 0.67 W/m^2K can be reduced to 0.55, and even 0.53 W/m^2K, if applying an IR reflective layer to one or both sides of the cavity, respectively.

4.4. Regarding Measured Heat Flow

The high temperatures on the interior cladding in the parapet area are a source of high heat losses (with the temperature difference being the driving force behind the heat flow).

The minimization of heat losses via thermal bridges and areas with poor thermal insulation must be considered in the future retrofit of the vehicle envelope.

Author Contributions: Conceptualization, R.H. and U.U.; Funding acquisition, U.U.; Investigation, W.R.; Methodology, C.G.; Project administration, R.H.; Supervision, C.G.; Writing—original draft, K.G.W.; Writing—review & editing, W.R. and K.G.W. All authors had equal contributions to this investigation. All authors have read and agreed to the published version of the manuscript.

Funding: This investigation was part of a project funded jointly by the Swiss Federal Office of Transport (FOT), the Raetian Railway (RhB), and Stadler Rail, all of Switzerland. Swiss Federal Office of Transport: BAV-Auftrag P-070.

Institutional Review Board Statement: Not applicable.

Informed Consent Statement: Not applicable.

Data Availability Statement: All data of the present investigation is available upon request.

Acknowledgments: The authors greatly acknowledge the support of the University of Basel by lending a portion of the measurement equipment, as well as sharing the corresponding measured data for the purpose of this study.

Conflicts of Interest: The authors declare no conflict of interest.

References

1. Energie PANORAMA—2020, Swiss Federal Statistical Office. Available online: https://www.bfs.admin.ch/bfs/en/home/statistics/energy.assetdetail.16704281.html (accessed on 20 September 2021).
2. Haller, G. Thermal Comfort in Rail Vehicles, Climatic Wind Tunnel Vienna. RTA Rail Tec Arsenal Fahrzeugversuchsanlage GmbH, 1210 Vienna, Austria. 2006. Available online: www.rta.co.at (accessed on 20 September 2021).
3. *EN 13129:2016*; Railway Applications—Air Conditioning for Main Line Rolling Stock—Comfort Parameters and Type Tests. CEN-CENELEC: Brussels, Belgium, 2006.
4. Liu, W.; Deng, Q.; Huang, W.; Liu, R. Variation in cooling load of a moving air-conditioned train compartment under the effects of ambient conditions and body thermal storage. *Appl. Therm. Eng.* **2011**, *31*, 1150–1162. [CrossRef]
5. Barone, G.; Buonomano, A.; Forzano, C.; Palombo, A. Enhancing trains envelope—heating, ventilation, and air conditioning systems: A new dynamic simulation approach for energy, economic, environmental impact and thermal comfort analyses. *Energy* **2020**, *204*, 117833. [CrossRef]
6. Bouvard, O.; Burnier, l.; Oelhafen, P.; Tonin, A.; Wüst, P.; Sidler, P.; Zweifel, G.; Schüler, A. Solar heat gains through train windows: A non-negligible contribution to the energy balance. *Energy Effic.* **2016**, *11*, 1397–1410. [CrossRef]
7. Beusen, B.; Degraeuwe, B.; Debeuf, P. Energy savings in light rail through the optimization of heating and ventilation. *Transp. Res. Part D* **2013**, *23*, 50–54. [CrossRef]
8. Chang, Y.; Lei, S.; Teng, J.; Zhang, J.; Zhang, L.; Xu, X. The energy use and environmental emissions of high-speed rail transportation in China: A bottom-up modeling. *Energy* **2019**, *182*, 1193–1201. [CrossRef]
9. Chow, W.K. Ventilation of enclosed train compartments in Hong Kong. *Appl. Energy* **2002**, *71*, 161–170. [CrossRef]
10. González-Gil, A.; Palacin, R.; Batty, P. Optimal energy management of urban rail systems: Key performance indicators. *Energy Convers. Manag.* **2015**, *90*, 282–291. [CrossRef]
11. Hofstädter, R.N.; Amaya, J.; Kozek, M. Energy optimal control of thermal comfort in trams. *Appl. Therm. Eng.* **2018**, *143*, 812–821. [CrossRef]
12. Lin, T.P.; Hwang, R.L.; Huang, K.T.; Sun, C.Y.; Huang, Y.C. Passenger thermal perceptions, thermal comfort requirements, and adaptations in short- and long-haul vehicles. *Int. J. Biometeorol.* **2010**, *54*, 221–230. [CrossRef] [PubMed]
13. Mastrullo, R.; Mauro, A.W.; Vellucci, C. Refrigerant alternatives for high-speed train A/C systems: Energy savings and environmental emissions evaluation under variable ambient conditions. *Energy Procedia* **2016**, *101*, 280–287. [CrossRef]
14. Ye, X.; Lu, H.; Li, D.; Sun, B.; Liu, Y. Thermal Comfort and Air Quality in Passenger Rail Cars. *Int. J. Vent.* **2004**, *3*, 183–192. [CrossRef]
15. Powell, J.P.; González-Gil, A.; Palacin, R. Experimental assessment of the energy consumption of urban rail vehicles during stabling hours: Influence of ambient temperature. *Appl. Therm. Eng.* **2014**, *66*, 541–547. [CrossRef]
16. Wernery, J.; Brunner, S.; Weber, B.; Knuth, C.; Koebel, M.M. Superinsulation materials for energy-efficient train envelopes. *Appl. Sci.* **2021**, *11*, 2339. [CrossRef]
17. Vetterli, N.; Menti, U.P.; Siedler, F.; Thaler, E.; Zweifel, G. Energy efficiency of railway vehicles. In Proceedings of the CISBAT, International Conference on Future Buildings and Districts—Sustainability from Nano to Urban Scale, Lausanne, Switzerland, 9–11 September 2015; Volume 2, pp. 955–960.
18. Oelhafen, P.; Tonin, A. Energy Efficiency of Heating, Ventilation, and Cooling in Public Transport (in German). Final Report for Project G055. Financially Supported by the Swiss Federal Office of Transport (FOT). 2018. Available online: https://www.bav.admin.ch/bav/de/home/suche.html#G055 (accessed on 20 September 2021).